CHAPTER 4

Wave-particle interactions with coherent magnetosonic waves

Lunjin Chen¹ and Jacob Bortnik²

¹Department of Physics, University of Texas at Dallas, Richardson, TX, United States

Contents

4.1	Introduction	99
4.2	Mathematical model	101
4.3	Wave-particle interactions with magnetosonic waves—coherent	105
4.4	Equatorially mirroring electrons	108
4.5	Bounce resonance diffusion theory	112
4.6	Summary	117
Acknowledgments		118
References		118

4.1 Introduction

Energetic electrons in the radiation belts undergo three quasi-periodic motions: gyration, bounce, and drift. The motions have distinct periods and each of them corresponds to an adiabatic invariant, referred to as the first, second, and third invariants, respectively (Schulz and Lanzerotti, 1974). The presence of plasma waves can violate one or more of the three invariants through wave-particle resonant interactions, leading to irreversible changes in electron phase space density (Thorne, 2010). The process of wave-particle interaction plays an important role in the variability of the radiation belt electrons. Much more attention has been paid to gyroresonance (see review by Albert et al., 2013, and references therein) and drift resonance interaction than bounce resonance, which can be responsible for the violation of the second invariant. Violation of the third invariant through drift interaction with ultralow frequency waves (e.g., Dai et al., 2013) can lead to radial diffusion, while violation of the first invariant through gyoresonance interaction can lead to pitch angle and energy scattering (e.g., Albert et al., 2013).

The investigation of bounce resonance started about five decades ago when Parker (1961) and Roberts and Schulz (1968) suggested that electrons can be subject to scattering by means of bounce resonance with hydrodynamic waves whose frequency is equal to multiples of electron bounce frequency. More recently, the idea of bounce

²Department of Atmospheric and Oceanic Sciences, University of California at Los Angeles, Los Angeles, CA, United States

resonance has gained increasing attention, in an attempt to explain the observed global coherent variability of the radiation belt electron fluxes (Kanekal et al., 2001; Shprits et al., 2007). Specifically, during geomagnetic storms, the radiation belt electron fluxes may vanish rapidly at all L-shells, indicating that electrons at all equatorial pitch angles are effectively scattered by waves. This is also true for equatorially mirroring electrons with equatorial pitch angles $\alpha_{eq} = 90$ degrees. However, those electrons are generally immune to the gyroresonance interaction, which requires a finite electron velocity component along the field line to satisfy the gyroresonance condition unless the relativistic mass correction is sufficient to reduce the electron gyrofrequency to match the wave frequency. However, when the relativistic correction factor is relatively small, it appears that the electrons with $\alpha_{eq} = 90$ degrees cannot be scattered by the waves with gyroresonance.

Among a variety of plasma waves in the magnetosphere, equatorial noise (Russell et al., 1969) is a potential candidate for bounce resonance with energetic electrons. Equatorial noise, also known as fast magnetosonic waves or ion Bernstein mode waves (Gary et al., 2010), consist of electromagnetic emissions confined within a few degrees of the equator (e.g., Santolík et al., 2004; Hrbáčková et al., 2015), occurring above the proton gyrofrequency f_{cv} and below the lower hybrid resonance frequency f_{LHR} . Magnetosonic wave frequencies typically range from a few Hz to ~ 100 Hz, and the low-frequency portion of the wave band is close to the bounce frequency of energetic electrons above hundreds of keV Shprits (2009). The dominant component of the magnetosonic wave's magnetic field is along the background magnetic field, leading to considerable magnetic mirror force along the electrons' bounce motion. The wave has average amplitudes of $\sim 50 \, \mathrm{pT}$ (Ma et al., 2013), but much more intense magnetosonic waves, with amplitudes up to ~1 nT, have also been reported (Tsurutani et al., 2014). Ring velocity distributions of the ring current energetic protons can excite these waves with nearly perpendicular wave normal angles (and hence near-perpendicular propagation directions) at multiples of the ion gyrofrequency (e.g., Perraut et al., 1982; Meredith et al., 2008; Chen et al., 2010, 2011). Discrete and harmonic spectral structures of magnetosonic waves have been reported during various satellite missions (e.g., Balikhin et al., 2015; Min et al., 2018).

These waves have also been shown to be effective for causing Landau resonance interactions, which are responsible for electron acceleration (Horne et al., 2007) and for inducing additional transit-time scattering (Bortnik and Thorne, 2010; Li et al., 2014). Both bounce resonant and Landau resonant scattering by magnetosonic waves have been proposed as mechanisms for the formation of butterfly distributions which require a depletion in equatorial and near-equatorially mirroring electron fluxes and/or enhancements of lower pitch angle electrons (Xiao et al., 2015; Li et al., 2016; Ma et al., 2016). Albert et al. (2016) demonstrated that a minimum phase space density at 90 degrees pitch angle for the inner radiation belt electrons can be reproduced by

the inclusion of cross pitch angle and energy diffusion without the presence of magnetosonic waves. In addition to diffusive interactions with magnetosonic waves, Maldonado et al. (2016) demonstrated that bounce resonance with coherent magnetosonic waves can lead to the observed rapid formation of butterfly distributions within seconds. In this chapter, we will cover recent developments in bounce resonance theory. We start with a test-particle model for studying the wave-particle interaction process, and then review Landau resonance, nonresonance, and bounce resonance with magnetosonic waves. Special attention is paid to the dynamics of equatorially mirroring electrons and coherent interactions over timescales longer than the bounce period. Finally, quasi-linear diffusion theory is reviewed, which accounts for the bounce resonance interactions with broadband waves.

4.2 Mathematical model

The mathematical model of nonrelativistic electron motion due to wave-particle gyroresonant interaction with oblique whistler waves was developed by Bell (1984), based on averaging the Lorentz force equations over the fast varying gyrophases and assuming a small wave magnetic amplitude as compared with the background magnetic field. A relativistic model was later generalized by Tao and Bortnik (2010) and Albert et al. (2013). Many various forms of the gyro-averaged equations have been used to study wave-particle gyroresonant interactions and Landau resonance (Bortnik and Thorne, 2010; Li et al., 2015; Hsieh and Omura, 2017). Such equations are also applicable for studying bounce resonance interactions (Chen et al., 2015; Maldonado et al., 2016; Li et al., 2015). Here we summarize the set of general gyro-averaged equations for electrons or ions, near an arbitrary resonance n, in a convention convenient for an arbitrary wave polarization and arbitrarily charged particles (electrons or ions):

$$\frac{dp_z}{dt} = -\frac{p_\perp^2}{2\gamma m B_0} \frac{dB_0}{dz} + g$$

$$\times \sum_j \left[\frac{q e^{i\phi_{j,n}}}{2} \left(\tilde{E}_{z,j} J_n + i \upsilon_\perp \tilde{B}_{-,j} J_{n+1} e^{i\psi_j} - i \upsilon_\perp \tilde{B}_{+,j} J_{n-1} e^{-i\psi_j} \right) + c.c. \right]$$
(4.1)

$$\frac{dp_{\perp}}{dt} = + \frac{p_{z}p_{\perp}}{2\gamma mB_{0}} \frac{dB_{0}}{dz} + g$$

$$\times \Sigma_{j} \left[\frac{qe^{i\phi_{j,n}}}{2} \left((\widetilde{E}_{-j} - i\upsilon_{z}\widetilde{B}_{-j}) J_{n+1}e^{i\psi_{j}} + (\widetilde{E}_{+,j} + i\upsilon_{z}\widetilde{B}_{+,j}) J_{n-1}e^{-i\psi_{j}} \right) + c.c. \right]$$
(4.2)

$$\frac{d\phi_{j,n}}{dt} = n\Omega - \omega_j + k_{z,j}\upsilon_z + \mathbf{k}_{\perp,j}\cdot\mathbf{v}_d + g$$

$$\times n\sum_j \left[\frac{qe^{i\phi_{j,n}}}{2} \left(\frac{\widetilde{E}_{-j} - i\upsilon_z \widetilde{B}_{-j}}{-ip_\perp} J_{n+1}e^{i\psi_j} + \frac{\widetilde{E}_{+,j} + i\upsilon_z \widetilde{B}_{+,j}}{ip_\perp} J_{n-1}e^{-i\psi_j} - \frac{\widetilde{B}_{z,j}}{\gamma m} J_n \right) + c.c. \right]$$
(4.3)

$$\frac{dz}{dt} = v_z \tag{4.4}$$

Here a field-aligned coordinate system is used, where z is oriented with the background magnetic field line B_0 and x and y are two perpendicular directions. Our background field B is assumed to be dipolar and z is the arc-distance along the field line measured from the geomagnetic equator; m is the charged particle's mass and q is the charge (with sign); γ is the Lorentz factor, and $p_z(\nu_z)$ and $p_\perp(\nu_\perp)$ are the particle's parallel and perpendicular momentum (velocity) components, respectively. v_d denotes particle drift velocity, that is, the velocity of the guiding center across the field line. The first terms on the right-hand side of Eqs. (4.1) and (4.2) represent the adiabatic variation due to background magnetic field, while the terms associated with summation denote the changes due to multiple wave effects. The subscript i denotes jth wave component with a corresponding frequency ω_i , parallel and perpendicular wave numbers, $k_{z,j}$ and $k_{\perp,j}$. \tilde{E} and \tilde{B} denote wave electric and magnetic complex amplitude, respectively. The wave components in a rotating coordinate system are denoted as $\tilde{B}_{\pm,j} = (\tilde{B}_{x,j} \pm i\tilde{B}_{y,j})/2$, $\tilde{E}_{\pm,j} = (\tilde{E}_{x,j} \pm i\tilde{E}_{y,j})/2$. The ratios among wave electric and magnetic complex amplitudes can be determined by the dispersion relation corresponding to a given wave mode with ω_i and k_i and local plasma parameters such as B_0 and plasma density. The local dispersion relation is solved for a plane wave of the form $\sim e^{ik_j \cdot r - i\omega_j t}$. The c.c. terms represent the complex conjugate of the wave force terms. The complex quantities are useful for implementing a general dispersion relation, not limited to the cold plasma dispersion relation often used previously. To be more general, the factor containing wave number azimuthal angle ψ_i is also retained. ψ_i is defined as the azimuthal angle of the wave vector $k_{\perp,i}$ with respect to the x axis.

The terms $J_n(\beta_j)$ are Bessel functions of the first kind with argument $\beta_j = \frac{k_\perp j p_\perp}{q B_0}$. The charged-particle gyrofrequency is $\Omega = q B_0/(\gamma m)$. These Bessel terms arise owing to the wave-phase variation along the gyromotion path, which is also known as the finite Larmor radius effect. It should be pointed out that $|J_0(\beta)| < 1$ and $|J_{+1}(\beta)| < \beta/2$, and therefore the Larmor radius effect produces a smaller driving force than the typical guiding-center approximation, which ignores the size of the Larmor radius. By letting β approach 0, Eqs. (4.1) and (4.2) can be

reduced to the guiding center approximation (e.g., Li et al., 2015) and the conservation of magnetic moment $\mu = p^2/(2mB_0)$. The term $\phi_{j,n}$ in Eq. (4.3) is the difference between the *j*th wave phase as seen by the center of the particle gyromotion and the *n*th multiple of the particle gyrophase. This difference takes into account the Doppler shift due to both parallel motion along the field line $(k_{z,j}v_z)$ and the perpendicular drift motion $(K_{\perp,j} \cdot v_d)$,

The scale factor $g(\lambda, t) = g_{\lambda}(\lambda)g_{t}(t)$, where λ is the magnetic latitude, $g_{\lambda}(\lambda) = \exp\left(-\frac{\lambda^{2}}{\lambda_{m}^{2}}\right)$ and

$$= \exp\left(-\frac{(t-t_1)^2}{\Delta t_1^2}\right) \text{for } t < t_1$$

$$g_t(t) = 1 \text{ for } t_1 \le t \le t_2$$

$$= \exp\left(-\frac{(t-t_2)^2}{\Delta t_2^2}\right) \text{for } t > t_2$$

 g_{λ} is introduced to represent latitudinal variation of the wave power with a latitudinal width of λ_{uv} , which is relevant for equatorially confined magnetosonic waves. The term g_t is introduced to account for temporal amplitude variation when particles drift through the wave fields over the localized azimuthal extent, that is, when particles enter or leave the field lines of interest. The waves turns on at $t=t_1$ and turns off at $t=t_2$. Launching test particles inside the wave field would induce unphysical scattering, in addition to the scattering due to the waves. Since we consider the interaction only along a fixed field line, it is implicitly assumed that the timescale of the wave existence $\tau=t_2-t_1$ is much less than drift period τ_d and is typically less than a few bounce periods τ_b .

Often one deals with a single primary resonance at a time, that is, only one possible solution for an integer n that is close to, if not equal to, the gyroresonance condition $n\Omega - \omega + k_z v_z = 0$. For magnetosonic waves, $|-\omega + k_z v_z| < |\Omega_e|$. Therefore, it is safe to consider n=0 only and as a result, electron trajectories are independent of the particle gyrophases, but the Larmor radius effect is still kept. For the case of n=0, the angle $\phi_{j,n=0}$ is simply the jth wave phase seen at the center of the gyration. The set of test particle Eqs. (4.1-4.4) with n=0 can be also used to investigate the bounce resonance interaction between electrons and magnetosonic waves for τ on the order of a few electron bounce periods. Here, we do not consider the effect of drift velocity v_d and consider only n=0, for which $\phi_{j,n=0}$; thus, Eqs. (4.1-4.4) are independent of gyration phases. Therefore, a wave number azimuthal angle of $\psi_j = 0$ is adopted (meaning k is on the plane containing k and k axes). It is worth noting that gyroresonant interactions (i.e., k0) depend on the gyrophases, and the value of k1 does affect the initial value of k2. As a consequence, particles' response to the wave field depends on k2.

Before discussing bounce resonance due to waves, we cover adiabatic bounce motion of electrons in the dipole magnetic field. The bounce motion is similar to motion in a potential well associated with background magnetic mirror, given by $\mu B_0(z)/\gamma^2$. The periods of relativistic bounce motion can be approximated by (e.g., Walt, 1994, Eq. 4.28)

$$\tau_b[\text{in s}] = 0.117 \times \frac{L\nu}{\epsilon} (1 - 0.4635 \sin^{0.75} \alpha_{eq}),$$

where v is the electron velocity, L is L-shell value, and c is the speed of light. Fig. 4.1 shows the electron bounce frequency, $f_b = 2\pi/\tau_b$, over a wide range of kinetic energies E in the magnetosphere; f_b ranges from a fraction of a Hz to 10 Hz and becomes greater for lower L values, higher equatorial pitch angles α_{eq} , and higher electron energies E. For ring current and radiation belt electrons (E > keV, 3 < L < 9), f_b is on the order of several Hz. Note that there exists a bounce frequency for exactly equatorially mirroring electrons ($\alpha_{eq} = 90$ degrees), although their trajectories remain on the equatorial plane. As noted in Chen et al. (2015), the behavior of equatorially mirroring electrons is analogous to particles at the bottom of the potential. Infinitesimal electric and magnetic perturbation, if any, will result in simple harmonic

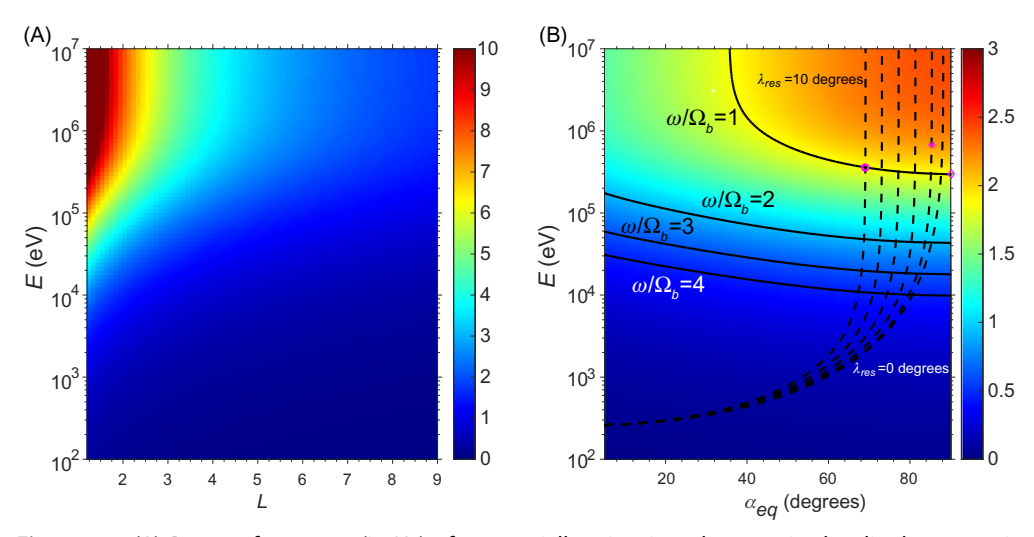


Figure 4.1 (A) Bounce frequency (in Hz) of equatorially mirroring electrons in the dipole magnetic field as a function of L-shell and kinetic energy. (B) Electron bounce frequency (in Hz) as a function of equatorial pitch angle α_{eq} and kinetic energy at L=6.6. The solid lines denote the bounce resonant condition $\omega=m_b\Omega_b$, where Ω_b is the angular frequency of electron bounce motion and m is an integer, 1, 2, 3, and 4. ω is set to Ω_b of electron with E=300 keV and $\alpha_{eq}=90$ degrees. The dashed lines denote Landau resonance condition $\omega-k_zv_z=0$ that takes place at magnetic latitude $\lambda_{res}=0$, 2, 4, 6, 8, and 10 degrees.

oscillation for those equatorially mirroring electrons with angular bounce frequency Ω_b given by $\Omega_b^2 = (\mu/\gamma^2 m_e) (d^2 B_0(z)/dz^2)|_{z=0}$. For a dipole field, bounce frequency for those electrons $\Omega_b^2 = (\mu/\gamma^2 m_e) (9B_0(z=0)/(LR_E)^2)$, where R_E is the Earth's radius.

4.3 Wave-particle interactions with magnetosonic waves—coherent

Here we deal with bounce resonant interactions between electrons and monochromatic magnetosonic wave fields. For a single wave, we simply remove the summation over j and suppress the subscript j in Eqs. (4.1-4.3). There are three possible nonadiabatic effects due to interaction with magnetosonic waves-Landau resonance, transit-time scattering, and bounce resonance. To illustrate these effects, we set L = 6.6, equatorial plasma density 50 cm⁻³, $t_1 = 0.4$ s, $\delta t_1 = 0.1$ s, $t_2 = \infty$ and wave frequency $\omega = 11 \text{ rad/s}$ with wave normal angle 89 degrees and latitudinal width $\lambda_w = 3$ degrees. In Fig. 4.1B, the dashed black lines denote the electrons that are in Landau resonance with the wave at various magnetic latitudes ($(\omega - k_z v_{z0}) = 0$), where v_{z0} is parallel velocity of the adiabatic motion, while solid black lines denotes the conditions when $\omega = m\Omega_b$, where m is an integer. Fig. 4.2A and C show trajectories of electrons with initial E = 354.8 keV and $\alpha_{eq} = 69.1 \text{ degrees}$ (marked by an asterisk in Fig. 4.1B) and random initial values of ϕ_0 . They are in Landau resonance at $\lambda_{res} = 2$ degrees but out of bounce resonance. Those electrons experience nonadiabatic changes in α_{eq} and E when electrons go through the resonant latitude because of slow variation of ϕ during Landau resonance (Eq. 4.3). These changes depend on the value of ϕ_0 , which is initially a random number. If the wave coherence does not hold longer than one bounce period ($\tau_c < \tau_b$), then the value of ϕ and thus the changes in momentum are randomized during the subsequent bounce. That is, the random change in momentum is independent of the random change during previous bounces, and therefore one should expect diffusive processes due to the Landau resonance.

Additional nonadiabatic changes occur because of equatorial confinement of magnetosonic wave power even when electrons are out of Landau resonance. This change is also known as transit-time scattering or nonresonance (Bortnik and Thorne, 2010). Fig. 4.2B and D shows the behavior of electrons with initial E and α_{eq} marked by the circle in Fig. 4.1B. There are net changes in α_{eq} and E whenever electrons pass through the equator. Such changes are induced when electrons rapidly pass through the edge of spatially confined wave power. Bortnik et al. (2015) analyzed the transit-time scattering in E and α_{eq} with the aid of two assumptions. First, the adiabatic variation of the particle velocity is ignored during equatorial crossing; that is, the zero-order parallel velocity ν_{z0} remains a constant when electrons pass through the wave field (Bortnik et al., 2015, Eq. 21), Second, the mirror latitudes are larger than the

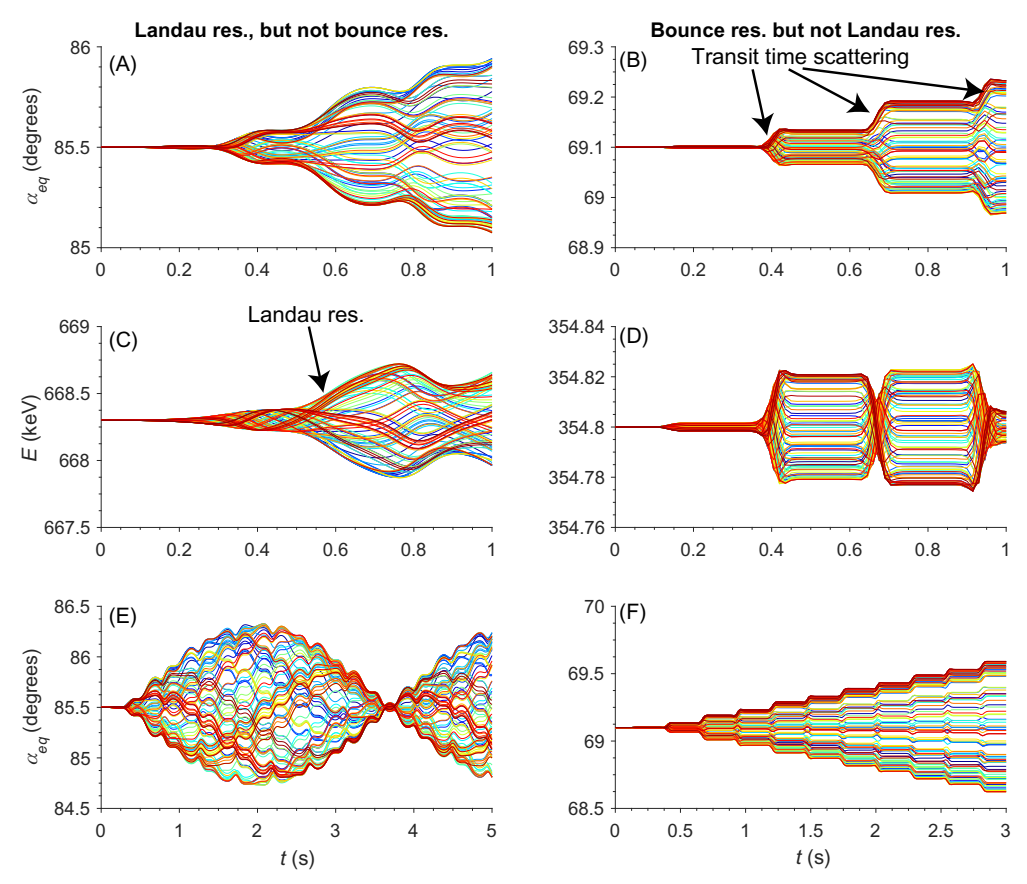


Figure 4.2 Simulated trajectories of electrons in a monochromatic magnetosonic wave field for electrons in Landau resonance with the magnetosonic wave but out of bounce resonance (*left column: A, C and E*) and for electrons out of Landau resonance but in bounce resonance (*left column: B, D and E*). Shown are electrons' equatorial pitch angle (*A, B*) and kinetic energy (*C, D*) as a function of time and pitch angle (*E, F*) for a longer time interval. The different colors represent different choices of random initial wave phases, ϕ_0 .

extent of the wave. Linear changes of the electron equatorial pitch angle (or *E*) due to a monochromatic wave follows

$$\Delta \alpha_{eq} \text{ or } \Delta E \sim \tau_{tr} \sin \phi_{eq} \exp \left(-\frac{(\omega - k_z \nu_{z0})^2 \tau_{tr}^2}{4}\right),$$
 (4.5)

where ϕ_{eq} is evaluated at the equator. The time to transit through the equatorial wave region, $\tau_{tr} = z_{w}/v_{z0}$, where z_{w} is the spatial width of wave power along the field line. The change is randomized for a random ϕ_{eq} and also depends on the change in wave phase during the passage $\Delta \phi \approx (-\omega + k_z v_{z0}) \tau_{tr}$ through the exponential factor.

If $|\Delta\phi|$ is large, then the effect vanishes, and for small $|\Delta\phi|$ ($<\sim$ 2), the net change occurs. The nonadiabatic effect favors the following two regimes: (1) for electrons near Landau resonance ($-\omega + k_z \nu_{z0} \approx 0$) and (2) for electrons transiting through the wave field rapidly (small τ_{tr}). For a large value of λ_{tr} , only electrons near Landau resonance are scattered. For a sufficiently small $\lambda_{\nu\nu}$ electrons, including those not in Landau resonance, can experience additional transit-time scattering. Such nonresonant scattering tends to broaden the regime of Landau resonant scattering. For $\tau_c < \tau_b$, one can expect transit time effects to induce diffusion in pitch angle and energy. The nonresonant effect has been also demonstrated in the interaction between subrelativistic/ relativistic electrons and parallel electromagnetic ion cyclotron (EMIC) wave packets (Chen et al., 2016), where the narrow spatial edge of the wave packet reduces the effective electron minimum energy of pitch angle scattering owing to interaction with gyromotion. For nonresonant interactions with EMIC wave packets, the nonresonant scattering becomes effective for the small phase change $|(-\omega - k_z \nu_z - \Omega_e) au_{
m tr}| < \sim 1$, where $au_{
m tr}$ is the time for electrons to pass through the spatial edge of the EMIC wave packet. The nonresonance vanishes when the phase change is larger. Such nonresonant effects associated with spatially confined wave packets broaden the interaction condition for gyroresonance and Landau resonance.

In addition to Landau resonance and transit-time effects, electrons can be in bounce resonance with the magnetosonic waves. Fig. 4.2F illustrates what happens during the bounce resonance over a few bounce periods. The electrons experience net nonadiabatic changes in α_{eq} and E due to nonresonant interactions. The net change depends on ϕ_{eq} . When in bounce resonance with waves of coherence of a timescale τ_c longer than τ_b , ϕ_{eq} remains unchanged during subsequent equatorial passage, and as a result, the same amount of nonadiabatic change is gained. In other words, the change $\Delta \alpha_{eq}$ is proportional to τ_c when in bounce resonance (as seen in Fig. 4.2F). Over the timescale comparable to τ_o although particles having different bounce phases have a different change in $\Delta \alpha_{eq}$, it is not a diffusive process. Fig. 4.3 shows the diffusive change and the advective change in α_{eq} and E as a function of time. During bounce resonance, the advective change remains small while the diffusive change increases linearly with time. If the wave phase is randomized after the coherent timescale τ_c then the effect of bounce resonance is randomized. As a result it becomes a random walk motion with each step per τ_c with standard deviation proportional to τ_c^2 . If the timescale of interest is $t \gg \tau_c$, then the process can be described as diffusive with averaged diffusion coefficients proportional to τ_c . That is, the longer the coherence timescale is for the bounce resonance, the stronger is the diffusion coefficient.

Now consider electrons that are in Landau resonance but not in bounce resonance (Fig. 4.2A, D, and E) for the case of $\tau_c \gg \tau_b$. Electrons experience a net change in momentum via Landau resonance during a bounce. Because the electrons are out of bounce resonance ($\omega \neq \Omega_b$), one would expect that they experience different

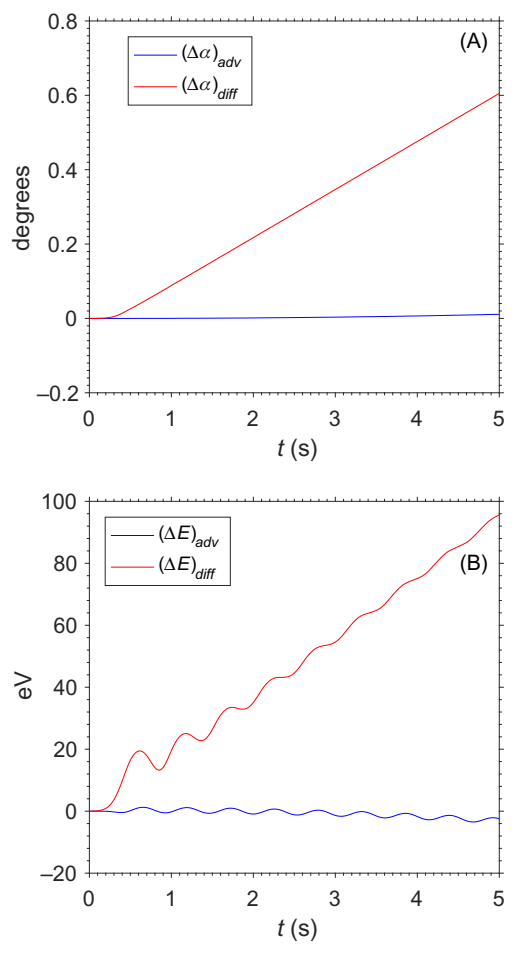


Figure 4.3 Advective (*blue*) and diffusive (*red*) transport in equatorial pitch angle (A) and kinetic (B) energy as a function of *t*, for electrons shown in the right column of Fig. 4.2.

momentum changes for each bounce, and then return to nearly initial values after a time period of $\sim \left[2\pi/(\Omega_b-\omega)\right]$ (as seen at $t\sim3.5$ seconds in Fig. 4.2E). Although the substantial oscillation in α_{eq} and E is induced by the Landau resonance, the change essentially vanishes at $t\sim3.5$ seconds after several bounce motions. Therefore, one would expect vanishing net effect for electrons not in bounce resonance when $\tau_c\gg\tau_b$.

4.4 Equatorially mirroring electrons

Equatorially and nearly equatorially mirroring electrons are generally immune to gyroresonance and Landau resonances that require a finite value of parallel velocity.

Those electrons also do not pass out of the wave-field region to experience transit-time scattering. Note that the mirror latitude of 3 degrees corresponds to $\alpha_{eq} = 83.6$ degrees. For these, $\nu_{z=0}$ is small and the adiabatic variation of $\nu_{z=0}$ cannot be ignored. As noted before, those electrons, much like staying on the bottom of the potential well, can exhibit bounce motion if perturbed by even infinitesimal electromagnetic fluctuations. One way to remove the electrons from the equatorial plane is through bounce resonance. Fig. 4.4 shows the responses of equatorially mirroring electrons (with initial conditions marked by the diamond in Fig. 4.1B) to the

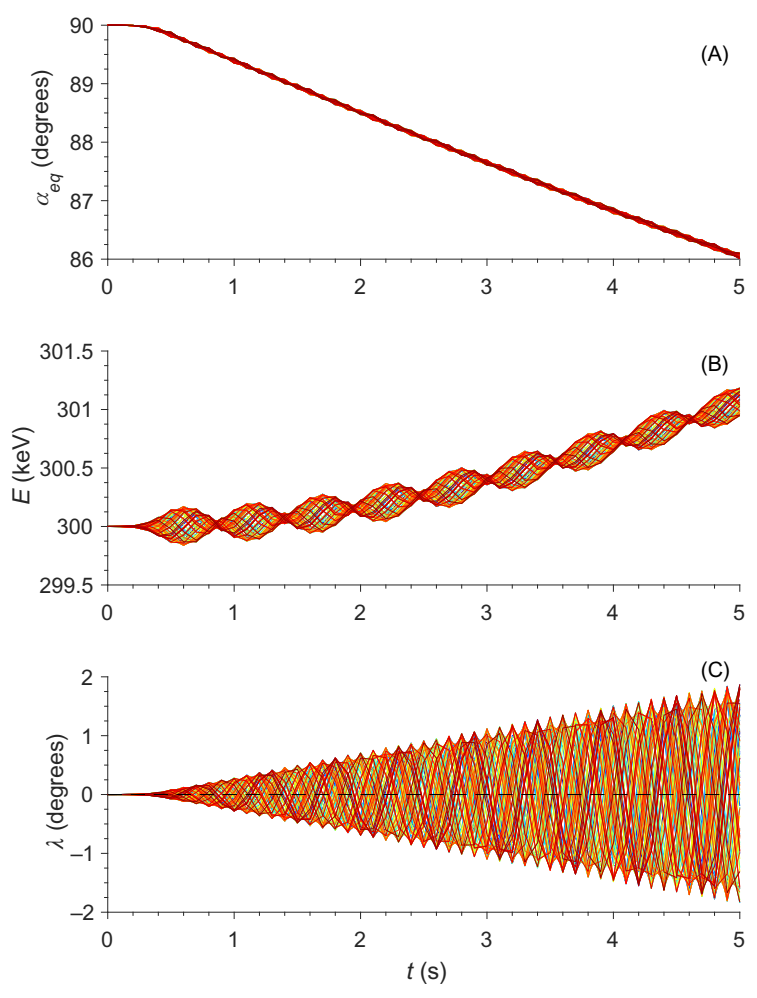


Figure 4.4 Illustration of equatorially mirroring electrons experiencing bounce resonance due to a monochromatic magnetosonic wave. Shown are electrons' equatorial pitch angles (A), kinetic energy (B), and magnetic latitudes as a function of time (C). Different colors represent different choices of random initial wave phases, ϕ_0 .

monochromatic wave described above. The dependence of electron responses to the initial phases ϕ_0 vanishes and the advective changes in α_{eq} (or E) dominate the diffusive changes. Those initially equatorially mirroring electrons experience a negative drift in α_{eq} and a positive drift E during the bounce resonance. Correspondingly they are removed from the equatorial plane with increasing mirror latitude (Fig. 4.4C). As shown by Chen et al. (2015), the response is sensitive to the ratio of wave frequency to electron bounce frequency. Fig. 4.5 demonstrates the bounce resonance that occurs when $\omega \sim n\Omega_b$, where n is an integer. No significant bounce resonance for $n \ge 4$ takes place for the choice of wave setup. For such high harmonic bounce resonance to take place, higher critical values of wave amplitude and wave number are required.

Eqs. (4.1–4.4) in Section 4.2 contain various physical components: relativistic motion, adiabatic effect due to the background magnetic field, the finite Larmor radius effects, transient scattering associated with latitudinal distribution $g(\lambda)$, bounce resonance, and Landau resonance (the $\omega - k_z v_z$ term). To gain more physical insight, a simplified nonlinear oscillation model in z for initially equatorially mirroring electrons is proposed by Chen et al. (2015), where changes in μ and in γ are ignored. Doing so allows the governing equations for the interaction between equatorially mirroring electrons and a monochromatic magnetosonic wave to be expressed as a nonlinear oscillation model, written as a second-order differential equation in a nondimensional form as:

$$d^2\tilde{z}/d\tilde{t}^2 + \tilde{z} + \frac{39}{18}\tilde{z}^3 = -\tilde{A}\sin(\tilde{\omega}\tilde{t} - \tilde{k}_z\tilde{z} + \phi_0)g(\lambda)$$
(4.6)

$$\tilde{z}|_{\tilde{t}=0} = d\tilde{z}/d\tilde{t}|_{\tilde{t}=0} = 0 \tag{4.7}$$

where nondimensional quantities $\tilde{z}=z/(LR_E)$, $\tilde{t}=\Omega_b t$, $\tilde{k}_z=k_z L R_E$, $\tilde{\omega}=\omega/\Omega_b$, and

$$\tilde{A} = \frac{\tilde{B}_z k_z L R_E}{9B_0} \frac{2J_1(\beta)}{\beta} + \frac{\tilde{E}_z J_0(\beta) e \gamma L R_E}{9\mu B_0}.$$
(4.8)

 Ω_b is the bounce frequency for electrons at $\alpha_{eq} = 90$ degrees. The normalized wave amplitude \tilde{A} contains the contribution from B_z^w and E_z^w . The \tilde{A} is equivalent to Eq. (4.11) of Roberts and Schulz (1968) in the limit of $\beta = 0$ ($J_0(\beta) = 1$ and $2J_1(\beta)/\beta = 1$) when the finite Larmor radius effect disappears. The \tilde{B}_z term, representing wave oscillatory magnetic mirror force, is generally much greater than the \tilde{E}_z term corresponding to the wave parallel electric force. The linear term and the nonlinear cubic term on the left-hand side of Eq. 4.6 arise from adiabatic changes, the first two terms on the left-hand side are responsible for harmonic bounce oscillations, and the nonlinear sine term on the right-hand side is driven by the wave with initial wave phase at the equator ϕ_0 and normalized wave amplitude at the equator.

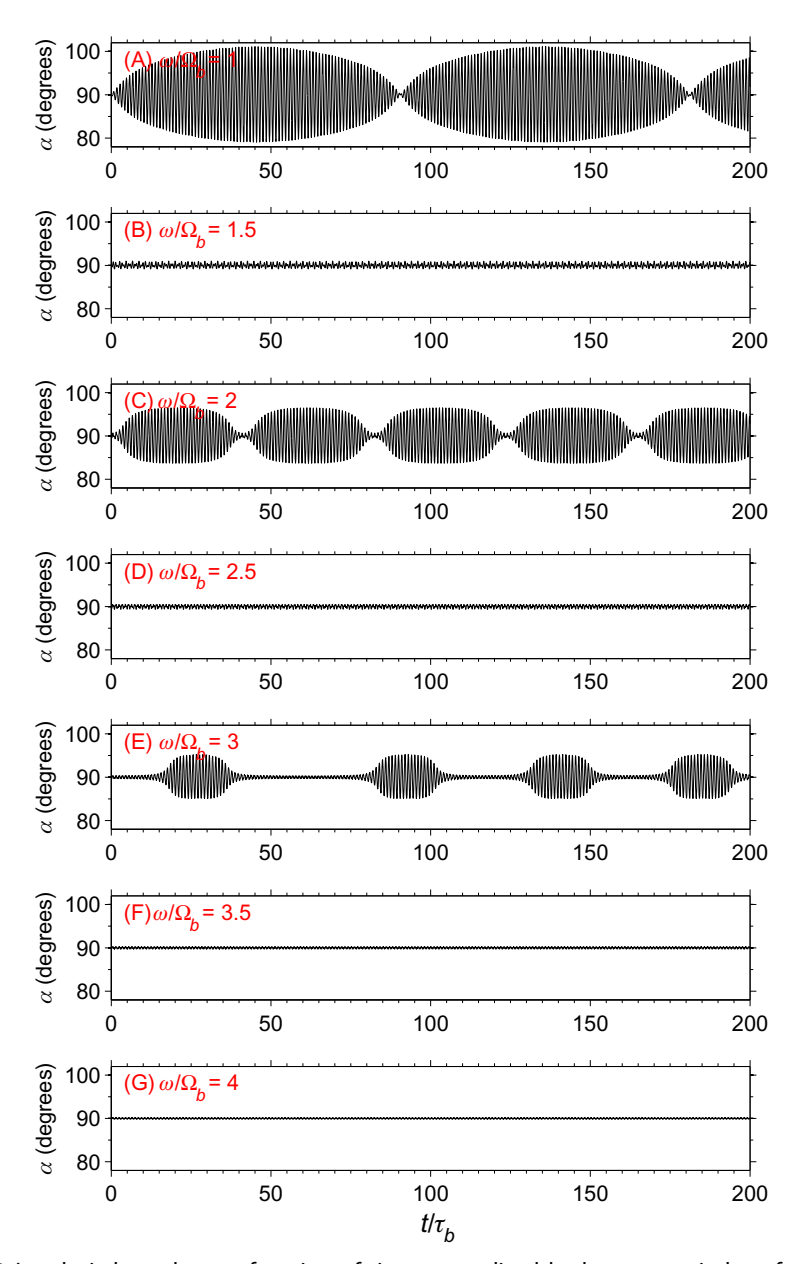


Figure 4.5 Local pitch angle as a function of time, normalized by bounce period τ_b , for electrons launched at the equator at L=6.6 with an initial pitch angle of 90 degrees and energy of 300 keV, driven by a monotonic magnetosonic wave with varying wave frequency: (A) 1.0 f_b , (B) 1.5 f_b , (C) 2.0 f_b , (D) 2.5 f_b , (E) 3.0 f_b , (F) 3.5 f_b , and(G) 4.0 f_b . Adapted from Fig. 4.2 of Chen, L., Maldonado, A., Bortnik, J., Thorne, R.M., Li, J., Dai, L., et al., 2015. Nonlinear bounce resonances between magnetosonic waves and equatorially mirroring electrons. J. Geophys. Res.

For $|\tilde{k}_z\tilde{z}| < 1$, Eq. (4.6) can be linearized as

$$d^2\tilde{z}/d\tilde{t}^2 + \tilde{z}(1 - \tilde{A}\tilde{k}_z\cos(\tilde{\omega}\tilde{t} + \phi_0)) = -\tilde{A}\sin(\tilde{\omega}\tilde{t} + \phi_0). \tag{4.9}$$

This linear equation is a driven Mathieu equation, permitting unstable solutions (i.e., bounce resonance solution) when $\tilde{\omega}$ is 2/q (where q is an integer). When bounce resonance occurs, the \tilde{z} amplitude increases and then nonlinear terms cannot be ignored and, therefore, this linear equation is not applicable.

For such coherent bounce interaction, equatorially mirroring electrons can experience a net drift toward smaller equatorial pitch angles, leading to a reduction of phase space density at $\alpha_{eq} = 90$ degrees. Maldonado et al. (2016) report a modulation of electron butterfly distribution (with a minimum of phase space density at $\alpha_{eq} = 90$ degrees) by varying the magnetosonic wave amplitude of a discrete spectrum. When the wave amplitude rises rapidly, an electron butterfly distribution forms. When the wave amplitude decays, the electron butterfly distribution vanishes. Such correlations demonstrate the response of electrons to the discrete magnetosonic spectrum. The direct test-particle simulation in the modeled single discrete frequency with a small frequency spread not only reproduces a rapid formation of butterfly distribution over the observed time scale of 10 seconds but also accounts for the energy range of the butterfly pitch angle distribution.

4.5 Bounce resonance diffusion theory

The response of electrons due to bounce resonance can be described through quasilinear diffusion with the assumption of weak turbulence with a small amplitude, random phase, and broadband spectrum. One can model the electron responses due to the weak turbulence by first solving the system of ordinary differential equations (Eqs. 4.1-4.4) with multiple waves. Unlike the coherent interactions discussed in Section 4.3, which involves single monochromatic waves, interactions with weak turbulence are realized by implementing multiple waves with a set of randomly selected initial wave phases and for electrons that were initially distributed at different bounce phases and then performing an ensemble average of the electron responses over the wave phases and bounce phases. Li et al. (2015) demonstrated that for broadband magnetosonic waves, the electron response can be treated as a diffusive process. Fig. 4.6A shows examples of electron trajectories with the same initial energy and equatorial pitch angle for different sets of initial wave phases. The equatorial pitch angle experiences random changes whenever there is bounce resonance with a frequency component of the magnetosonic wave broadband spectrum. The deviation of electron equatorial pitch angles from simulated responses over an ensemble of initial wave phases increases linearly over time (Fig. 4.6B), corresponding to a diffusion

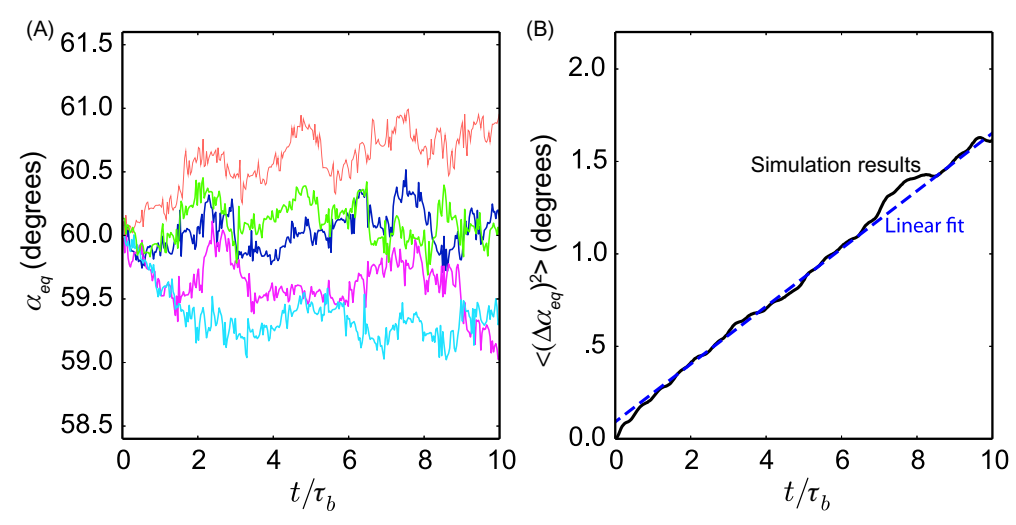


Figure 4.6 (A) Changes in α_{eq} of five randomly selected electrons with initial $\alpha_{eq} = 60$ degrees, represented by different colors. (B) The evolution of corresponding $<(\Delta\alpha_{eq})^2>$ with time. The blue line denotes the corresponding linear fitting. Adapted from Fig. 4.1 of Li, X., Tao, X., Lu, Q., Dai, L., 2015. Bounce resonance diffusion coefficients for spatially confined waves. Geophys. Res. Lett. 42 (22), 9591–9599, doi:10.1002/2015GL066324.

process in equatorial pitch angle for the electron population. The slope of the deviation with respect to time, representing diffusion coefficient, can be obtained from numerical test-particle simulation.

Theoretical diffusion coefficients have been derived under different assumptions. Roberts (1968) and Schulz and Lanzerotti (1974) assume a guiding-center approximation for electron motion (i.e., for small β and conservation of magnetic moment) and a flat latitudinal distribution of magnetohydrodynamic wave power distribution. The diffusion coefficient formula is applied to magnetosonic waves (Shprits, 2016) following the same method. Li et al. (2015) extended the formula to a wave power distribution that exists and is flat only over a specified magnetic latitude range, taking into account the equatorial confinement of magnetosonic wave power. Maldonado and Chen (2018) further extend the bounce resonance diffusion formula to a more realistic magnetosonic wave model, with the finite Larmor radius effect, a more realistic Gaussian latitudinal distribution instead of the square distribution used in Li et al. (2015), and potential violation of magnetic moment μ are included. The finite Larmor radius effect takes place when the wavelength of those magnetosonic waves is comparable to, and shorter than, the gyroradius of energetic electrons (i.e., the ratio of electron gyroradius to perpendicular wavelength, $\rho_{o}k_{\perp} > \sim 1$). This is especially true for the interaction between nearly perpendicularly propagating magnetosonic waves and energetic radiation belt electrons. For $\rho_{\sigma}k_{\perp} > -1$, the first adiabatic invariant can

be violated, because electrons experience significant spatial variation of wave fields over one gyration. One should use the set of Eqs. 4.1—4.4 for the electron responses, instead of a simplified guiding center approximation. Furthermore, the observed latitudinal wave power distribution shows a narrow peak near the equator instead of being flat (Němec et al., 2005). These factors are valuable for quantifying the effects of magnetosonic waves on electron scattering. Therefore, we review a general bounce resonant diffusion theory with the above three factors included; a detailed derivation can be found in Li et al. (2015) and Maldonado and Chen (2018).

Three assumptions are made to obtain the diffusion coefficients. (1) Assume unperturbed adiabatic motion, that is, $z = z_m \sin(\Omega_b t + \theta_0)$ and thus $v_z = z_m \Omega_b \cos(\Omega_b t + \theta_0)$, where θ_0 denotes the initial bounce phase of the electron motion. This assumption is different from the assumption made in Bortnik and Thorne (2010) for evaluating transit-time scattering, who assume no adiabatic variation when passing through the wave field. Since the waves are confined near the equator, we assume that v_\perp and p_\perp of the wave terms in Eqs. (4.1) and (4.2) remain unchanged as the equatorial values of the zero-order adiabatic motion. (2) Assume linear perturbation is much less than the zero-order motion, that is, wave field is so weak that no significant change in α_{eq} and E occurs after a bounce cycle. This assumption may not be valid for equatorially mirroring electrons, whose zero-order adiabatic motion is not well defined. (3) Consider multiple wave components with a Gaussian latitudinal distribution of wave power and adopt Eqs. (4.1) and (4.2) with finite Larmor radius effects included.

With those assumptions, one can integrate Eqs. (4.1) and (4.2) along the unperturbed bounce motion, to obtain α_{eq} and E due to multiple magnetosonic waves over time τ and obtain the change of α_{eq} and E as a function of time τ ,

$$\Delta E = \tau \sum_{\text{integer } x_j > 0} \exp\left(i\phi'_{j0}\right) \tilde{B}_{z,j} X_E + c.c. \tag{4.10}$$

and

$$\Delta \alpha_{eq} = \tau \sum_{\text{integer } x_i > 0} \exp\left(i\phi'_{j0}\right) \tilde{B}_{z,j} X_{\alpha} + c.c. \tag{4.11}$$

where $\phi'_{j0} = \phi_{j,0} + x_j \theta_0$, $x_j = \omega_j / \Omega_b$, Ω_b is electron bounce frequency, and the two complex numbers are given by

$$X_{E} = \sum_{k_{2}} I_{k2} e^{-c_{0}} \left[\frac{1}{4} \sum_{l_{1} = x_{j} \pm 2k_{2}} - iq \frac{\tilde{E}_{\gamma,j}}{\tilde{B}_{z,j}} \upsilon_{\perp 0} J_{1} J_{l_{1}} + \frac{1}{8} \sum_{l_{1} = x_{j} \pm 2k_{2} \pm 1} z_{m} \Omega_{b} q \frac{\tilde{E}_{z,j}}{\tilde{B}_{z,j}} J_{0} J_{l_{1}} \right]$$

and

$$X_{\alpha} = \sum_{k_2} I_{k_2} e^{-c_0} \left[\frac{1}{4} \sum_{l_1 = x_j \pm 2k_2} iq \frac{\tilde{E}_{\gamma,j}}{\tilde{B}_{z,j}} J_1 J_{l_1} \frac{-p_{z_0}}{p_0^2} \right]$$
(4.12)

$$+\frac{1}{8}\sum_{l_{1}=x_{i}\pm2k_{2}\pm1}-\frac{z_{m}\Omega_{b}q\upsilon_{\perp0}}{\upsilon^{2}p_{z0}}\frac{\tilde{E}_{z,j}}{\tilde{B}_{z,j}}J_{0}J_{l_{1}}+\frac{z_{m}\Omega_{b}iq}{p_{z0}}\frac{\tilde{B}_{x,j}}{\tilde{B}_{z,j}}J_{1}J_{l_{1}}]$$
(4.13)

The argument of J_0 and J_1 , $k_\perp p_{\perp,0}/qB_0$, measures the ratio of gyromotion radius and perpendicular wavelength. Similarly, the argument for J_{l_1} , $k_{z,j}z_m$, measures the ratio of bounce amplitude and parallel wavelength. The argument for I_{k_2} is $c_0 = \lambda_m^2/2\lambda_w^2$, measuring the ratio of bounce amplitude and the field-aligned width of equatorially confined waves. λ_m is the electron mirror magnetic latitude.

A few points are noted from Eqs. (4.10) and (4.11). First, the wave amplitudes \tilde{B} and \tilde{E} represent their equatorial values and can be normalized by any component of the wave electromagnetic fields, \tilde{B}_z , in these two equations. The ratios among the wave field components are obtained by local dispersion relation at the equator. Second, ΔE and $\Delta \alpha_{eq}$ are proportional to τ when electrons are subject to bounce resonance, which requires integer values of x_j (= ω_j/Ω_b). In other words, only waves in bounce resonance lead to ΔE and $\Delta \alpha_{eq}$, while other waves produce no net change. (3) ΔE and $\Delta \alpha_{eq}$ are oscillatory because of the term $\exp(i\phi'_{j0})$, where ϕ'_{j0} is a linear combination of initial wave phase (ϕ_{j0}) and initial bounce phase (θ_0). The ensemble average of $<(\Delta \alpha_{eq})$ > over the two phases vanishes while the ensemble average of $<(\Delta \alpha_{eq})^2$ > is proportional to the wave power.

Diffusion coefficients due to bounce resonance with broadband magnetosonic waves can be obtained through

$$D_{\alpha\alpha} = \left\langle \frac{\left(\Delta \alpha_{eq}\right) \left(\Delta \alpha_{eq}\right)}{2\tau} \right\rangle = 2 \sum_{\text{integer } x_i > 0} P_{Bz} \left(f = x_j f_b \right) \Re \left(X_{\alpha} X_{\alpha}^* \right) \tag{4.14}$$

$$D_{\alpha E} = \left\langle \frac{\left(\Delta \alpha_{eq}\right)(\Delta E)}{2\tau} \right\rangle = 2 \sum_{\text{integer } x_j > 0} P_{Bz} \left(f = x_j f_b \right) \Re \left(X_\alpha X_E^* \right)$$
(4.15)

$$D_{EE} = \left\langle \frac{(\Delta E)(\Delta E)}{2\tau} \right\rangle = 2 \sum_{\text{integer } x_j > 0} P_{Bz} (f = x_j f_b) \Re \left(X_E X_E^* \right)$$
(4.16)

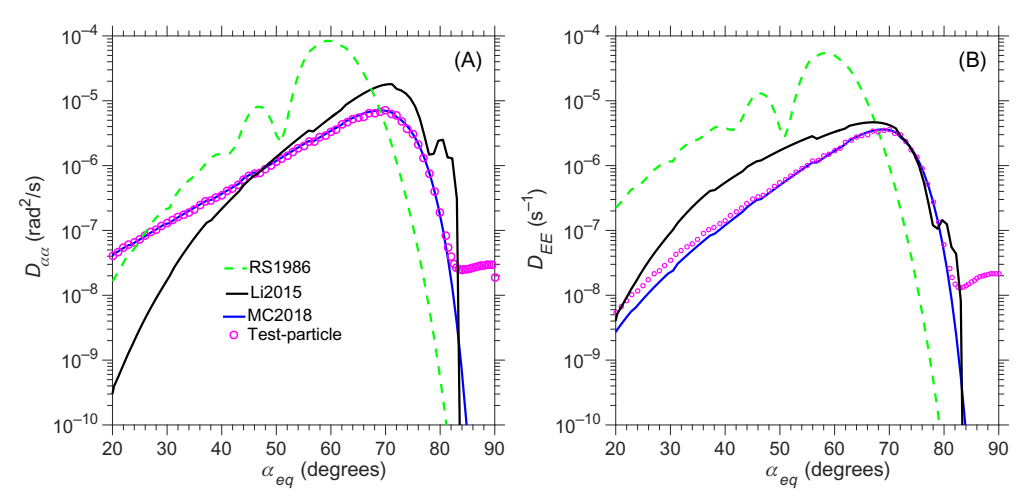


Figure 4.7 Comparison of (A) pitch angle and (B) energy diffusion coefficients among Roberts and Schulz (1968) (*green dashed line*), Li et al. (2015) (*black solid line*), and Maldonado and Chen (2018) (*blue solid line*). Also shown are the diffusion coefficients derived from the numerical test-particle simulation (*magenta circles*). Adapted From Fig. 4.1 of Maldonado, A.A., Chen, L., 2018. On the diffusion rates of electron bounce resonant scattering by magnetosonic waves. Geophys. Res. Lett., 45, 3328–3337. doi:10.1002/2017GL076560.

where the brackets represent the ensemble average, P_{Bz} represents the power spectrum density of the wave magnetic parallel component, in units of T^2/Hz , as a function of wave frequency f, the subscript * denotes complex conjugate, and \Re represents real part.

Fig. 4.7 shows a comparison among the three formulas as a function of electron pitch angles developed by Roberts and Schulz (1968), Li et al. (2015), and Maldonado and Chen (2018) for electrons at L = 4.5 with kinetic energy E = 1 MeV. The three curves in Fig. 4.7 have the same plasma-frequency-to-electron-gyrofrequency ratio $f_{pe}/f_{ce} = 3$, and the same magnetosonic wave spectral parameters. The magnetosonic wave parameters are adopted from Horne et al. (2007). The waves assume a rootmean-squared amplitude 218 pT, a single wave normal angle of 89 degrees, and a Gaussian frequency spectrum of $B(\omega) \propto exp(-(\omega - \omega_m)^2/\delta\omega^2)$, where $\omega_m = 3.49 \times 10^{-3} \Omega_e$, and $\delta \omega = 8.86 \times 10^{-4} \Omega_e$. The frequency range of the spectral density distribution spans from the lower cutoff $\omega_{LC} = 2 \times 10^{-3} \Omega_e$ to the upper cutoff $\omega_{UC} = 5 \times 10^{-3} \Omega_e$. The RS1968 and Li2015 curves adopt guiding center approximation (with conservation of magnetic moment and zero Larmor radius) but assume different latitudinal distributions of wave power, being flat throughout the field line for the former while being flat over only a limited $\lambda \leq 3$ degrees for the latter. One can see that compared with RS1968, the Li2015 curve expects less scattering over low α_{eq} < 67 degrees owing to the lack of wave power at high latitude (λ > 3 degrees) and higher scattering for 67 degrees $\leq \alpha_{eq} \leq 87$ degrees because of additional scattering when those electrons transit through the wave edge at $\lambda=3$ degrees. The MC2018 formula adopts test-particle equations in Eqs. (4.1) and (4.2), which considers finite Larmor radius and does not assume magnetic moment conservation, and a more realistic Gaussian latitudinal distribution of wave power centered at the equator and latitudinal width of 3 degrees. When comparing MC2018 with Li2015, one can notice two discrepancies. First, MC2018 produces less scattering at 45 degrees $<\alpha_{eq}<85$ degrees due to the finite Larmor radius effect, which tends to be more significant for large α_{eq} and to weaken the wave force. Second, MC2018 enhances scattering at low $\alpha_{eq}<45$ degrees. The enhancement is attributed to the additional scattering caused by the change in magnetic moment μ when electrons experience rapid spatial variation of wave fields over gyration.

To verify the analytic diffusion coefficient, the test particle simulation using Eqs. (4.1) and (4.2) is performed. For a given initial energy and pitch angle, the simulation is performed for 100 randomly selected initial bounce phases and 101 sets of randomly assigned initial wave phases. Ensemble average of this 100×101 set of simulation results is performed to obtain the numerical diffusion coefficients (shown by magenta circles in Fig. 4.7). One can see that diffusion coefficients derived from numerical test-particle simulation are in close agreement with the theoretical MC2018 curve. One discrepancy between the numerical coefficients and the analytic ones occurs for α_{eq} near 90 degrees, which may be due to the breakdown of the second assumption and to the additional advective responses (see Section 4.4). Dependences of the diffusion coefficients on various plasma and waves parameters are explored systematically in Maldonado and Chen (2018).

Tao and Li (2016) further consider wave normal angle distribution to examine the bounce resonant scattering and find that the inclusion of wave normal angle distribution favors pitch angle scattering for equatorially and nearly equatorially mirroring electrons, which is later validated using guiding-center test-particle simulations (Li and Tao, 2017). Bounce resonance diffusion theory has also been applied to other types of plasma waves, for example, EMIC waves below ion gyrofrequency (Cao et al., 2017a) and the low-frequency portion of plasmaspheric hiss waves (Cao et al., 2017b).

4.6 Summary

Bounce resonance interaction with magnetosonic waves has been developed both in terms of coherent interaction and quasi-linear scattering. The bounce resonance diffusion or advection by magnetosonic waves could be an important mechanism to account for dynamics of equatorially and nearly equatorially mirroring electrons. Those newly developed coefficients are expected to be incorporated into existing Fokker—Planck framework for radiation belt modeling.

Acknowledgments

This work was supported by NSF grants 1405041 and 1702805 through the Geospace Environment Modeling program, an AFOSR grant FA9550-16-1-0344, and NASA grants NNX15AF55G and NNX17AI52G. JB gratefully acknowledges the joint Department of Energy and the National Science Foundation grant DE-SC0010578, which was awarded to UCLA through the NSF/DOE Plasma Partnership program and also NASA grant NNX16AG21G.

References

- Albert, J.M., Tao, X., Bortnik, J., 2013. Aspects of nonlinear wave—particle interactions. In: Summers, D., Mann, I.R., Baker, D.N., Schulz, M. (Eds.), Dynamics of the Earth's Radiation Belts and Inner Magnetosphere, Geophysical Monograph Series. American Geophysical Union, pp. 255–264. Available from: https://doi.org/10.1029/2012GM001324.
- Albert, J.M., Starks, M.J., Horne, R.B., Meredith, N.P., Glauert, S.A., 2016. Quasi-linear simulations of inner radiation belt electron pitch angle and energy distributions. Geophys. Res. Lett. 43 (6), 2381–2388. https://agupubs.onlinelibrary.wiley.com/doi/abs/ 10.1002/ 2016GL067938.
- Balikhin, M.A., Shprits, Y.Y., Walker, S.N., Chen, L., Cornilleau-Wehrlin, N., Dandouras, I., et al., 2015. Observations of discrete harmonics emerging from equatorial noise. Nat. Commun. 6, 7703.
- Bell, T.F., 1984. The nonlinear gyroresonance interaction between energetic electrons and coherent VLF waves propagating at an arbitrary angle with respect to the earth's magnetic field. J. Geophys. Res. 89, 905–918.
- Bortnik, J., Thorne, R.M., 2010. Transit time scattering of energetic electrons due to equatorially confined magnetosonic waves. J. Geophys. Res. 115, 7213.
- Bortnik, J., Thorne, R.M., Ni, B., Li, J., 2015. Analytical approximation of transit time scattering due to magnetosonic waves. Geophys. Res. Lett. 42 (5), 1318–1325. Available from: https://doi.org/10.1002/2014GL062710.
- Cao, X., Ni, B., Summers, D., Bortnik, J., Tao, X., Shprits, Y.Y., et al., 2017a. Bounce resonance scattering of radiation belt electrons by H + band emic waves. J. Geophys. Res. Space Phys. 122 (2), 1702–1713. Available from: https://doi.org/10.1002/2016JA023607. 2016JA023607.
- Cao, X., Ni, B., Summers, D., Zou, Z., Fu, S., Zhang, W., 2017b. Bounce resonance scattering of radiation belt electrons by low-frequency hiss: comparison with cyclotron and landau resonances. Geophys. Res. Lett. 44 (19), 9547–9554. Available from: https://doi.org/10.1002/2017GL075104.
- Chen, L., Thorne, R.M., Jordanova, V.K., Horne, R.B., 2010. Global simulation of magnetosonic waves instability in the storm time magnetosphere. J. Geophys. Res. 115, A11222. Available from: https://doi.org/10.1029/2010JA015707.
- Chen, L., Thorne, R.M., Jordanova, V.K., Thomsen, M.F., Horne, R.B., 2011. Magnetosonic wave instability analysis for proton ring distributions observed by the LANL magnetospheric plasma analyzer. J. Geophys. Res. 116, 3223.
- Chen, L., Maldonado, A., Bortnik, J., Thorne, R.M., Li, J., Dai, L., et al., 2015. Nonlinear bounce resonances between magnetosonic waves and equatorially mirroring electrons. J. Geophys. Res 120, 6514–6527. Available from: https://doi.org/10.1002/2015JA021174.
- Chen, L., Thorne, R.M., Bortnik, J., Zhang, X.-J., 2016. Nonresonant interactions of electromagnetic ion cyclotron waves with relativistic electrons. J. Geophys. Res. Space Phys. 121 (10), 9913–9925. Available from: https://doi.org/10.1002/2016JA022813. 2016JA022813.
- Dai, L., Takahashi, K., Wygant, J.R., Chen, L., Bonnell, J., Cattell, C.A., et al., 2013. Excitation of poloidal standing Alfvén waves through drift resonance wave—particle interaction. Geophys. Res. Lett. 40, 4127—4132.
- Gary, S.P., Liu, K., Winske, D., Denton, R.E., 2010. Ion Bernstein instability in the terrestrial magnetosphere: linear dispersion theory. J. Geophys. Res. 115, 12209.

- Horne, R.B., Thorne, R.M., Glauert, S.A., Meredith, N.P., Pokhotelov, D., Santolík, O., 2007. Electron acceleration in the Van Allen radiation belts by fast magnetosonic waves. Geophys. Res. Lett. 34, L17107.
- Hrbáčková, Z., Santolík, O., Němec, F., Macúšová, E., Cornilleau-Wehrlin, N., 2015. Systematic analysis of occurrence of equatorial noise emissions using 10 years of data from the Cluster mission. J. Geophys. Res. 120, 1007–1021.
- Hsieh, Y.-K., Omura, Y., 2017. Nonlinear dynamics of electrons interacting with oblique whistler mode chorus in the magnetosphere. J. Geophys. Res. Space Phys. 122 (1), 675–694. Available from: https://doi.org/10.1002/2016JA023255. 2016JA023255.
- Kanekal, S., Baker, D., Blake, J., 2001. Multisatellite measurements of relativistic electrons: global coherence. J. Geophys. Res. 106 (A12), 29721–29732.
- Li, J., Ni, B., Xie, L., Pu, Z., Bortnik, J., Thorne, R.M., et al., 2014. Interactions between magnetosonic waves and radiation belt electrons: comparisons of quasi-linear calculations with test particle simulations. Geophys. Res. Lett. 41 (14), 4828–4834.
- Li, J., Bortnik, J., Xie, L., Pu, Z., Chen, L., Ni, B., et al., 2015. Comparison of formulas for resonant interactions between energetic electrons and oblique whistler-mode waves. Phys. Plasmas 22 (5), 052902.
- Li, J., Ni, B., Ma, Q., Xie, L., Pu, Z., Fu, S., et al., 2016. Formation of energetic electron butterfly distributions by magnetosonic waves via landau resonance. Geophys. Res. Lett. 43 (7), 3009–3016. Available from: https://doi.org/10.1002/2016GL067853. 2016GL067853.
- Li, X., Tao, X., 2017. Validation and analysis of bounce resonance diffusion coefficients. J. Geophys. Res. Space Phys. 123, 104–113. Available from: https://doi.org/10.1002/2017JA024506.
- Li, X., Tao, X., Lu, Q., Dai, L., 2015. Bounce resonance diffusion coefficients for spatially confined waves. Geophys. Res. Lett. 42 (22), 9591–9599. Available from: https://doi.org/10.1002/ 2015GL066324.
- Ma, Q., Li, W., Thorne, R.M., Angelopoulos, V., 2013. Global distribution of equatorial magnetosonic waves observed by themis. Geophys. Res. Lett. 40 (10), 1895—1901. Available from: https://doi.org/10.1002/grl.50434.
- Ma, Q., Li, W., Thorne, R.M., Bortnik, J., Kletzing, C.A., Kurth, W.S., et al., 2016. Electron scattering by magnetosonic waves in the inner magnetosphere. J. Geophys. Res. Space Phys. 121 (1), 274–285. Available from: https://doi.org/10.1002/2015JA021992.
- Maldonado, A.A., Chen, L., 2018. On the diffusion rates of electron bounce resonant scattering by magnetosonic waves. Geophys. Res. Lett. 45, 3328–3337. Available from: https://doi.org/10.1002/2017GL076560.
- Maldonado, A.A., Chen, L., Claudepierre, S.G., Bortnik, J., Thorne, R.M., Spence, H., 2016. Electron butterfly distribution modulation by magnetosonic waves. Geophys. Res. Lett. 43 (7), 3051–3059. Available from: https://doi.org/10.1002/2016GL068161. 2016GL068161.
- Meredith, N.P., Horne, R.B., Anderson, R.R., 2008. Survey of magnetosonic waves and proton ring distributions in the Earth's inner magnetosphere. J. Geophys. Res. 113, 6213.
- Min, K., Liu, K., Wang, X., Chen, L., Denton, R.E., 2018. Fast magnetosonic waves observed by Van Allen Probes: testing local wave excitation mechanism. J. Geophys. Res. Space Phys. Available from: https://doi.org/10.1002/2017JA0248672169-94022017JA024867.
- Němec, F., Santolík, O., Gereová, K., Macúšová, E., de Conchy, Y., Cornilleau-Wehrlin, N., 2005. Initial results of a survey of equatorial noise emissions observed by the Cluster spacecraft. Planet. Space Sci., 53, 291–298.
- Parker, E.N., 1961. Effect of hydromagnetic waves in a dipole field on the longitudinal invariant. J. Geophys. Res. 66 (3), 693–708. Available from: https://doi.org/10.1029/JZ066i003p00693.
- Perraut, S., Roux, A., Robert, P., Gendrin, R., Sauvaud, J., Bosqued, J., et al., 1982. A systematic study of ULF waves above F/H plus/ from GEOS 1 and 2 measurements and their relationships with proton ring distributions. J. Geophys. Res. 87, 6219–6236.
- Roberts, C.S., 1968. Cyclotron-resonance and bounce-resonance scattering of electrons trapped in the earth's magnetic field. In: Earth's Particles and Fields. J. Geophys. Res., 73 (23), 7361–7376, https://doi.org/10.1029/JA073i023p07361.

- Roberts, C.S., Schulz, M., 1968. Bounce resonant scattering of particles trapped in the earth's magnetic field. J. Geophys. Res. 73 (23), 7361–7376.
- Russell, C.T., Holzer, R.E., Smith, E.J., 1969. OGO 3 observations of ELF noise in the magnetosphere. 1. Spatial extent and frequency of occurrence. J. Geophys. Res. 74, 755–777.
- Santolík, O., Nemec, F., Gereová, K., Macúšová, E., Conchy, Y., Cornilleau-Wehrlin, N., 2004. Systematic analysis of equatorial noise below the lower hybrid frequency. Ann. Geophys. 22, 2587–2595.
- Schulz, M., Lanzerotti, L.J., 1974. *Particle Diffusion in the Radiation Belts*. Physics and Chemistry in Space, Vol. 7. Springer-Verlag, Berlin, Heidelberg, pp. 62–65, Ch. II.4.
- Shprits, Y., Kondrashov, D., Chen, Y., Thorne, R., Ghil, M., Friedel, R., et al., 2007. Reanalysis of relativistic radiation belt electron fluxes using crres satellite data, a radial diffusion model, and a kalman filter. J. Geophys. Res. 112 (A12).
- Shprits, Y.Y., 2009. Potential waves for pitch-angle scattering of near-equatorially mirroring energetic electrons due to the violation of the second adiabatic invariant. Geophys. Res. Lett. 36, 12106.
- Shprits, Y.Y., 2016. Estimation of bounce resonant scattering by fast magnetosonic waves. Geophys. Res. Lett. 43 (3), 998–1006. Available from: https://doi.org/10.1002/2015GL066796. 2015GL066796.
- Tao, X., Bortnik, J., 2010. Nonlinear interactions between relativistic radiation belt electrons and oblique whistler mode waves. Nonlinear Process. Geophys. 17 (5), 599–604. Available from: https://www. nonlin-processes-geophys.net/17/599/2010/.
- Tao, X., Li, X., 2016. Theoretical bounce resonance diffusion coefficient for waves generated near the equatorial plane. Geophys. Res. Lett. 43, 7389–7397.
- Thorne, R.M., 2010. Radiation belt dynamics: the importance of wave-particle interactions. Geophys. Res. Lett. 37 (22).
- Tsurutani, B.T., Falkowski, B.J., Pickett, J.S., Verkhoglyadova, O.P., Santolik, O., Lakhina, G.S., 2014. Extremely intense ELF magnetosonic waves: a survey of polar observations. J. Geophys. Res. 119, 964–977.
- Walt, M., 1994. Introduction to geomagnetically trapped radiation. Camb. Atmos. Space Sci. Ser. 10, 10.Xiao, F., Yang, C., Su, Z., Zhou, Q., He, Z., He, Y., et al., 2015. Wave-driven butterfly distribution of Van Allen belt relativistic electrons. Nat. Commun. 6, 8590.